Fish Physiol Biochem (2021) 47:1149–1164
https://doi.org/10.1007/s10695-021-00964-3

Metabolism and antioxidation regulation of total flavanones from *Sedum sarmentosum* Bunge against high-fat diet-induced fatty liver disease in Nile tilapia (*Oreochromis niloticus*)

Kai Yu · Kai Huang · Zhanyang Tang · Xiuyun Huang · Linlin Sun · Linxing Pang · Cuiqin Mo

Received: 21 July 2020 / Accepted: 7 May 2021 / Published online: 18 June 2021

Abstract Diet-induced fatty liver is a considerable threaten to fish aquaculture due to the popularity of the high-fat diet (HFD) feeding. Our study aims to investigate the effects of flavanones from *Sedum sarmentosum* Bunge (FSSB) on the liver function to identify a potential treatment for HFD-induced fatty liver disease. Physiological and pathological indicators were tested in the liver of Nile tilapia (*Oreochromis niloticus*) and results showed parameters including lipid metabolites, redox parameters, and inflammatory factors could be adequately restored to normal level by addition of 150 mg/kg FSSB to HFD. Proteomics analysis was performed in liver tissues from tilapia with normal diet (ND), HFD, and HFD+FSSB. Totally, 51 upregulated proteins and 77 downregulated proteins were identified in HFD groups and 67 proteins of them were restored after treated with FSSB. Bioinformatics analysis showed that differentially expressed proteins (DEPs) in HFD+FSSB150 group compared with HFD group are mainly enriched in acety-CoA metabolic process, adenosine-triphosphate (ATP) biosynthetic process, lipid metabolic process, and phospholipid metabolic process. The dysregulated proteins were involved in peroxidosome proliferators-activated receptor (PPAR) signaling pathway, fat digestion and absorption, and immune system. The quantitative real-time PCR (qRT-PCR) assay further revealed that the expression of *GST*, *PPARα*, *PPARγ*, and multiple-inflammatory cytokines could be also reversed in HFD group under the treatment of 150 mg/kg FSSB. Our findings demonstrated FSSB is efficient for the treatment of fatty liver disease through regulation of lipid metabolism and antioxidation in Nile tilapia, providing a new treatment of non-alcoholic fatty liver disease (NAFLD) in fish aquaculture.

Keywords Fatty liver disease · FSSB · Proteomics · *Oreochromis niloticus* · Lipid metabolism · PPAR

Highlights We investigated hepatoprotective effects of flavanones from Chinese herb on fatty liver disease in tilapia through the regulation of lipid metabolism, antioxidation, and immunity.

K. Yu · K. Huang (✉) · Z. Tang · X. Huang · L. Sun · L. Pang · C. Mo
College of Animal Science and Technology, Guangxi University, No. 100 East Daxue Road, Nanning 530004, China
e-mail: kaihuangnn1@163.com

Z. Tang (✉)
Guangxi Academy of Fishery Science, Nanning 530021, China
e-mail: 13712896731@qq.com

Introduction

Fatty liver is one of the diseases that affect the pathological changes of the liver, which has threatened the aquacultures worldwide. Unbalanced nutrition, overdue metamorphic feeding, and unscientific management of culture, especially the excessive dietary lipid level, are likely to cause fatty liver disease in aquaculture. Fish with fatty liver disease exhibit reduced growth rate, disease resistance, and eventually lead to serious economic losses to aquaculture industry. Great efforts have been paid to study the physiological and pathogenetic

effects of high dietary intake of carbohydrates in zebrafish (*Danio rerio*), medaka (*Oryzias latipes*), and blunt snout bream (*Megalobrama amblycephala*) (Goessling and Sadler 2015; Lieschke and Currie 2007; Matsumoto et al. 2010; Prisingkorn et al. 2017). These effects can influence liver size and lipid accumulation and cause the oneset of nonalcoholic fatty liver disease (NAFLD). Tao et al. and Tian et al. confirmed that excessive dietary lipids could break the balance of lipolysis and lipogenesis, lead to lipid deposition, and alter fatty acid composition and antioxidant enzyme activities in Nile tilapia (*Oreochromis niloticus*) (Tao et al. 2018; Tian et al. 2015). Excess lipid intake induces oxidative stress, negative regulation of disease resistance in a wide range of fish species, such as turbot (*Scophthalmus maximus*), blunt snout bream, and zebrafish (Adjoumani et al. 2017; Jia et al. 2017; Landgraf et al. 2017). However, the physiological mechanisms of fatty liver disease have not been reported in Nile tilapia.

According to previous studies, fatty liver has been characterized by multiple pathological and functional disorder of the liver in mammalia, including insulin resistance, lipid deposition, raising oxidative stress, and inflammation genesis (Kitade et al. 2017; Lau et al. 2017). Fatty liver disease was found to be facilitated by fatty acid absorption from blood via L-FABP, a transporter of fatty acid, and transformation of redundant proteins and sugars (Furuhashi and Hotamisligil 2008). While the degradation pathway or transfer of triglyceride and cholesterol was blocked, fatty liver developed, and fatty degeneration occurred. Many researches focused on the molecular pathogenesis of fatty liver development in fish have been reported. For example, Prisingkorn et al. employed transcriptomics and metabolomics to study the effects of a high-carbohydrate diet on blunt snout bream. Their results indicated that the regulated genes associated with insulin signaling pathway, such as *IL6*, resulted in insulin resistance in hepatocytes, pathological changes in the liver, and the development of NAFLD (Prisingkorn et al. 2017). A deep sequencing study of miRNAs of normal and high-fat diet (HFD) fed blunt snout bream showed that lipid metabolism-related genes, such as ones encoding fatty-acid synthase, stearoyl-CoA desaturase, fetuin-B, and Cyp7a1, constructed a lipid metabolism regulatory network regulated by miRNA (Zhang et al. 2014). Furthermore, Qiang et al. found that miR-122 functions as a negative regulator of SCD and mediates hepatic fat metabolism in tilapia (Qiang et al. 2018). These studies focus on the phenotype and gene expression differences resulting from liver fat imbalances. However, the protein expression levels, the dynamic profiles of functional proteins, and pathways in the development of this disease are rarely reported.

Many traditional Chinese herbal medicines have been found to be efficient treatments for NAFLD; for example, extracts from *Sedum sarmentosum* Bunge (SSB) (Huang et al. 2018b) and *Rhizoma Alismatis* (Du et al. 2018). SSB is a traditional herb that has been employed for the treatment of chronic viral hepatitis due to its hepatoprotective characteristics (He et al. 1998). In our previous study, SSB extract showed comprehensive protection against nonalcoholic steatohepatitis (Huang et al. 2018b). However, the influences of particular natural bioactive SSB on HDF-induced fatty liver disease of fish is still unclear.

Therefore, in the present study, we investigated the effects of total flavanones, the main active constituents from SSB, on tilapia phenotypes using a HFD-induced tilapia model of fatty liver disease. Furthermore, a high-throughput proteomic study based on the combination of iTRAQ labeling and LC-MS/MS was utilized to screen potential mechanism-related functional proteins.

Materials and methods

Tilapia breeding

All protocols, care, and handling of fish in this study were approved by the Animal Ethics Committee of Guangxi University, in accordance with IASP Guidelines for the Use of Laboratory Animals in Research. The tilapias (0.85 ± 0.01g) were purchased from Guangxi Wuming Aquaculture Breeding Center (Wuming, China). After acclimatization in laboratory conditions in dechlorinated tap water for 7 days, 300 healthy fish (4.08 ± 0.15 g) were first cultured on a HFD for 8 weeks for model establishment and 60 healthy fish were cultured on a normal diet (ND) for control. Then, the model fish were randomly divided into five groups and supplemented with different concentrations of total flavanones from *Sedum sarmentosum* Bunge (FSSB), including 0 mg/kg (FSSB0), 50 mg/kg (FSSB50), 100 mg/kg (FSSB100), 150 mg/kg (FSSB150), and 200 mg/kg (FSSB200) for 6 weeks. The control group was cultured for an additional 6 weeks in normal diet. Total

flavanones from SSB were extracted by 80% ethanol and then purified through macroporous absorption resin and polyamide resin (Lin et al. 2020). Main ingredients of FSSB detected by LC-MS/MS are listed in Table S1. Formulation and proximate composition details of the experimental diets are described in Table S2. During the course of the treatment, the water temperature was maintained at 20–25 °C, the pH was dominated at 7.2 ±0.1, and the dissolved oxygen was controlled at 6.51 ±0.43mg/L. At the completion of treatment, the fish were euthanized with MS-222 after a 24-h fast period.

Evaluation of fatty liver model and drug efficiency

After treatment, the fish bodies, liver tissues, and intraperitoneal fat were weighted to evaluate growth performance, including weight gain rate, specific growth rate, feed efficiency, hepatosomatic index, and intraperitoneal fat index. For the detection of crude liver fat content, fresh tissues were performed by Soxhlet extraction using SZC-C Fat Analyzer (Xianjian instrument Co., Ltd., Shanghai, China). For model evaluation, tissue sections from the fish livers were used. The NAFLD Activity Score (NAS) rules (Table S3) were adopted to judge whether the model was successful based on three standards: (1) the ratio of hepatic steatosis; (2) the number of inflammatory lesions; and (3) the probability of fat vacuolar balloon degeneration (Fan 2010). Nine livers in groups ND, HFD, and HFD+FSSB150 were used for proteomic analysis, respectively. Serum samples used for parameter detection were separated as previous described (Zuo et al. 2012). Serum samples and the remaining liver samples were stored at −80 °C for subsequent assays.

Hematoxylin and eosin staining, and transmission electron microscope observation

Hematoxylin and eosin (H&E) staining was used to detect the pathological changes of the liver tissue in fish. The liver tissues were fixed in 10% formaldehyde (Sangon Biotech Co., Ltd., Shanghai) for 48 h and were washed with running water; dehydrated with different concentrations of ethanol. The tissue was then immersed in wax, embedded in paraffin (Sangon Biotech Co., Ltd., Shanghai), and sliced to a thickness of 4 μm. The slides were placed in a 65 °C constant temperature oven for 30 min, xylene I for 15 min, and then xylene II (Sangon Biotech Co., Ltd., Shanghai) for 15 min. The dewaxed sections were soaked in different concentrations of ethanol for 5 min and rinsed with tap water for 10 min. The sections were then stained with H&E. The cell nuclei were stained with hematoxylin (Sigma-Aldrich, St. Louis, MO, USA) for 5 min and the cytoplasm was stained using eosin (Sigma-Aldrich, St. Louis, MO, USA) for 1–2 min. The stained sections were dehydrated with pure alcohol and examined under a light microscope (ECLIPSE Ni, Nikon, USA). Areas of lipid vacuoles were quantified relatively by Image-Pro Plus 6.0 software. The observation of ultrastructure in liver tissue by transmission electron microscope (TEM) was conducted according to previously described by Huang et al. (Huang et al. 2018a). Briefly, the liver samples were fixed with 2.5% glutaraldehyde and then in 1% phosphate-buffered osmium tetroxide. Tissues were sectioned into ultrathin sections using EM UC7 Ultramicrotome (Leica, Wetzlar, Germany) after being dehydrated and embedded. For observation, sections were double-stained with uranyl acetate and lead citrate, and captured with TEM (Tecnai G^2 20 TWIN, FEI, Hillsboro, USA).

Protein extraction and digestion

For proteomic analysis, liver samples from nine individual fish of each group were divided into three replicates. The samples were first pulverized using liquid nitrogen, transferred to a 1.5-mL centrifuge tube, and sonicated three times on ice in Urea buffer (8 M Urea, 2 mM EDTA, 10 mM DTT) combined with 1% PMSF using a high-intensity ultrasonic processor (ATPIO, Xo-650D). The remaining debris was removed by centrifugation at 12,000×*g* at 4°C for 10 min. Protein concentration was determined using a Bradford kit (Beyotime, Shanghai, China) according to the manufacturer's instructions. For digestion, 100 μg protein from each sample was first reduced with 10 mM DTT at 37 °C for 60 min and then alkylated in darkness with 25 mM μl IAM at room temperature for 30 min. The solution was applied to 10 kDa MWCO centrifugal filter units to remove impurities before being diluted with 100 mM triethyl ammonium bicarbonate (TEAB), and then centrifuged for 30 min at 10,000 rpm. Finally, digestion was achieved using Sequencing Grade Modified Trypsin, first with a 50:1 mass ratio incubated at 37 °C overnight and then at 100:1 for a second digestion at 37 °C for 4 h.

Peptide isobaric labeling and fractionation

After digestion, peptides were desalted by Strata X SPE column and vacuum-dried. Peptides were reconstituted in 100 μL of 100 mM TEAB and processed according to the manufacturer's protocol for 8-plex isobaric tags for relative and absolute quantification (iTRAQ) kits. Briefly, one unit of iTRAQ reagent was added to peptide solution after thawing and dissolved in 50 μL isopropanol. The peptide mixtures were incubated for 1 h at 25 °C, pooled, and dried by vacuum centrifugation. The dried and labeled peptides were reconstituted with high performance liquid chromatography (HPLC) solution A (2%ACN, pH 10) and then fractionated by HPLC using high pH reverse-phase C18 column (Waters XBridge BEH130, 3.5 μm, 4.6 × 250 mm). The peptides were first separated with a gradient of 8–35% acetonitrile at pH 10 at a speed of 0.5 ml/min over 60 min, then combined into 18 fractions and dried by vacuum centrifugation. Afterwards, the peptide fractions were desalted using Ziptip C18 according to the manufacturer's instructions and finally vacuum dried and kept at −20 °C until MS analyses were performed.

High-resolution LC-MS/MS analysis

The LC-MS/MS analysis was performed by EASY-nLC 1000 system (Proxeon) coupled to Q Exactive (Thermo Fisher Scientific). Trypsin digestion fractions were reconstituted in 0.1% fatty acid (FA) and loaded onto a reversed-phase analytical column (Acclaim PepMap® RSLC C18, 2 μm, 100Å, 50 μm × 15 cm), of which the gradient consisted of an increase from 2 to 100% solvent B (0.1% FA in 95% ACN) over 58 min at a constant flow rate of 300 nL/min on an EASY-nLC 1000 system. The eluent was sprayed via NanoSpray Ionization source at 2.0 kV and then analyzed by tandem mass spectrometry (MS/MS) using Q Exactive. The mass spectrometer was operated in data-dependent mode, automatically switching between MS and MS/MS. Full-scan MS spectra (from m/z 350 to 1800) were acquired in the Orbitrap with a resolution of 70,000. Ion fragments were detected in the Orbitrap at a resolution of 17,500 and the 20 most intense precursors were selected for subsequent decision tree-based ion trap HCD fragmentation at a collision energy of 28 in the MS survey scan with 15.0s dynamic exclusion.

Quantitative real-time PCR verification

Several crucial genes involved in PPAR signaling pathway, fat digestion and absorption process, and inflammatory cytokines were validated by quantitative real-time PCR (qRT-PCR). Total RNA was isolated from the liver tissues using Trizol reagent (Invitrogen) according to the manufacturer's instructions. All primers were designed and synthesized by Yingbio (Shanghai, China) and are shown in Table S4. Briefly, complementary DNA (cDNA) was created using the RevertAid First Strand cDNA synthesis kit (Thermo Fisher Scientific) and amplified with FastStart Universal SYBR Green Master (Rox) and QuantStudio 6 Flex Real-Time PCR System (Thermo Fisher Scientific) according to the instruction. Quantification of glyceraldehyde-3phosphate dehydrogenase (GAPDH) served as an endogenous control. Gene expression was determined by the $2^{-\Delta\Delta Cq}$ method.

Enzyme-linked immunosorbent assay

An enzyme-linked immunosorbent assay (ELISA) was used to detect changes in inflammatory factors of liver tissues from Nile tilapia in the ND, HFD, and HFD+FSSB150 groups. Frozen liver tissue samples of Nile tilapia from each group were fully homogenized in presence of protease inhibitors (Sigma-Aldrich) and centrifuged at 8000×*g* for 10 min at 4°C. The homogenization fluid was used for tested inflammatory factor using the ELISA kits (Meimian, Jiangsu, China). These experiments were performed following the manufacturer's instructions.

Data processing

The resulting MS/MS raw data were searched against with the *Oreochromis niloticus* proteome database (Uniprot database, Taxon identifier: 8128, include 26757 protein sequences) use the SEQUEST software for protein identification and quantification. For the search parameters, carbamidomethylation (C) was set as a fixed modification, and oxidation (M) and acetylation in N-Term were set as variable modifications. The searches were performed using a peptide mass tolerance of 20 ppm and a product ion tolerance of 0.05 Da, resulting in 5% false discovery rate (FDR).

Bioinformatics analysis

The protein sequence was compared to eukaryotic orthologous groups (KOG) from complete orthologous genome databases to annotate the KOG functions. These were classified by Gene Ontology Annotation (GOA) based on three categories: biological process (BP), cellular component (CC), and molecular function (MF). The GOA annotation proteome was derived from the UniProt-GOA database (www.http://www.ebi.ac.uk/GOA/). The Kyoto Encyclopedia of Genes and Genomes (KEGG) database was used to annotate protein pathways. Its online service tool, KEGG Automatic Annotation Server (KAAS), was used to annotate the proteins' KEGG database description and map the annotation results onto the KEGG PATHWAY database using KEGG Mapper.

Functional enrichment

A two-tailed Fisher's exact test was used to test the Gene Ontology (GO) KEGG pathway enrichment of the differential expression proteins against all other identified proteins. Correction for multiple hypothesis testing was carried out under standard FDR control methods with a corrected p-value, where $p < 0.05$ was considered significant.

Expression-based clustering and enrichment-based clustering for protein groups

Expression-based and functional enrichment-based clustering was used to explore potential relationships between different protein groups by comparing special protein functions (such as KEGG pathway). Firstly, we obtained a functional enrichment analysis along with the associated p-values. Secondly, we sorted those categories enriched in at least one of the protein groups with $p < 0.05$. This filtered p-value matrix was transformed by the function $x = -\log10$ (p-value). Thirdly, the x-values of each functional category were z-transformed. These z-scores were clustered by one-way hierarchical clustering (Euclidean distance, average linkage clustering). Finally, clusters were visualized by a heatmap using the "pheatmap" function in R.

Statistical analysis

Data were presented as the mean and standard deviation (SD). Statistical differences among the three groups were analyzed by one-way ANOVA using SPSS software (Statistical Package for Social Sciences, SPSS Corporation, Chicago, USA). Paired comparisons of means were performed using the unpaired two-tailed Student's t-test, where $p < 0.05$ was considered statistically significant, and $p < 0.001$ was considered highly statistically significant.

Results

Evaluation of fat liver disease and growth performance of Nile tilapia fed with different diets

According to NAS rules, we compared the livers of Nile tilapia fed on ND, HFD, and HFD+FSSB150. The results showed that, after 8 weeks, the score of HFD group was 7.1 (Table S3), which can been defined as significant NASH. However, because the score of liver sections in ND and HFD+FSSB150 groups was < 3.0, NASH can be excluded. In addition, the growth performance of Nile tilapia fed on different diets is shown in Table S5. It was evident that HFD-fed Nile tilapia showed reduced weight gain and specific growth rates compared to the ND group. In contrast, after administration of HFD+FSSB150, these indexes were increased compared with the HFD group. The feed efficiency, hepatosomatic index, intraperitoneal fat index, and crude liver fat content of the HFD group were higher than the ND group. Conversely, by supplementing HFD with FSSB150, these indexes could be restored to a relatively normal level.

Effect of FSSB on lipid deposition of hepatocyte in Nile tilapia

H&E staining was used to examine pathological changes in liver tissues of ND, HFD, and HFD+FSSB150 groups. The results showed that the liver tissues of the ND group showed normal histological structure. In comparison with the ND group, the liver tissues of the HFD group had aggravated swollen cells, obvious cavitation, vacuolar lipid droplets, and displaced nuclei, which suggests the development of fatty liver disease. Administration of FSSB150 could reduce the degree of

cavitation and nuclei arrangement in the hepatocyte, and the liver tissues showed relatively normal structure (Fig. 1a–c). H&E staining also allowed for the quantification of the area ratio for lipid droplets, the results of which were consistent with those determined by observation (Fig. 1d). Moreover, TEM assays revealed that the hepatocyte ultrastructure of the HFD group was changed compared to the ND group and an increased amount of lipid droplets, accumulated glycogen, and the loss of cristae in swollen mitochondria were observed in the HFD group. However, supplementation of FSSB150 helped to restore the abnormal mitochondria and eliminate lipid droplets.

Protective effect of FSSB on the liver of Nile tilapia

To evaluate the effect of FSSB treatment, we detected the indexes of physiological and pathological changes in the livers of specimens from ND, HFD, and HFD+FSSB150 groups. The detection of serum parameters showed differences between the different diets. The contents of triglyceride (TG) and total cholesterol (TC) were significantly increased in the HFD group compared with the ND group, while they were decreased in the HFD+FSSB150 group compared with the HFD group (Fig. 2a, b). The ratio of high-density lipoprotein (HDL)/low-density lipoprotein (LDL) cholesterol was lower in the HFD group than in the ND group, while the supplement of FSSB150 could reverse this change (Fig. 2c). These results demonstrate that lipid accumulation induced by HFD could be improved by the supplement of FSSB. Additionally, to determine the antioxidant effects of FSSB, the protein levels of malondialdehyde (MDA) and activity of total superoxide disumutase (T-SOD) and catalase (CAT) in liver tissues were evaluated. In comparison with the ND group, the protein level of MDA was significantly enhanced, while the activity of T-SOD and CAT was remarkably reduced in the HFD group (Fig. 2d–f). However, the supplement of FSSB150 could reverse these changes. Activities of GPT and GOT showed a decrease under the treatment of FSSB150 (Fig. 2g, h). The levels of tumor necrosis factor (TNF)-α and interleukin (IL)-8 were dramatically increased, while the level of IL-10 was significantly decreased in the HFD group compared with the ND group (Fig. 2i–k). In contrast, these changes were reversed after FSSB150 treatment.

Summary statistics for the proteomic profile

We used the gel-free proteomic strategy to explore proteomic shifting in FSSB-treated Nile tilapia. In total, 4485 proteins were identified and 2856 proteins were quantified. The heatmap showed that protein expression in the HFD+FSSB150 group was more similar to the ND group, and less like the HFD group (Fig. 3a). In addition, 77 proteins were downregulated and 51 proteins were upregulated in the HFD group compared to the ND group. In comparison with the HFD group, 135 proteins were downregulated and 199 proteins were upregulated in the HFD+FSSB150 group. The 20 most upregulated and downregulated proteins were clearly seen on the volcano diagram (Fig. 3b, c). Moreover, the Venn diagram showed that 67 proteins showed opposite changes to the two comparisons mentioned above. Specifically, 27 proteins were downregulated and 40 proteins were upregulated in the HFD+FSSB150 group compared with the HFD group (Fig. 3d).

KOG and GO functional analysis of differentially expressed proteins (DEPs)

To predict putative protein functions, KOG and GO analysis was performed. The DEPs were divided into 23 categories. In the comparison of the HFD and ND groups, and comparison of HFD+FSSB150 and HFD groups, the top 3 classified KOG functions were both signal transduction mechanisms, general function prediction only, and posttranslational modification, protein turnover, and chaperones (Fig. 4a, 4b). GO functional analysis revealed that fructose-6-phosphate metabolic process, lipid localization, and fatty acid metabolic process were main GO terms between HFD and ND groups (Fig. 4c). The DEGs between HFD+FSSB150 and HFD were mainly enriched in acetyl-CoA biosynthetic process, ATP biosynthetic process, phospholipid metabolic process, and lipid metabolic process (Fig. 4d). DEPs annotated to acetyl-CoA metabolism, ATP biosynthesis, fat digestion and absorption, and lipid metabolism in the comparison of HFD versus ND and HFD+FSSB150 versus HFD are listed in Table 1.

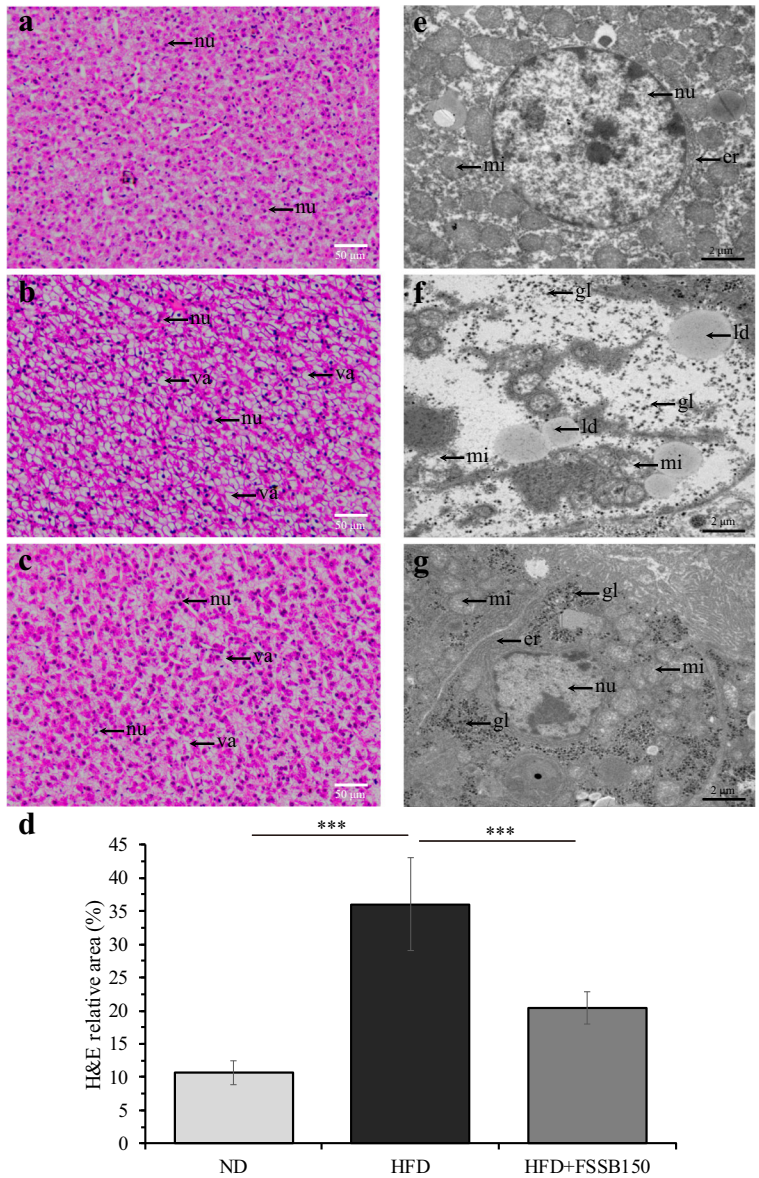

Fig. 1 FSSB attenuates lipid accumulation induced by HFD. (a–c) H&E staining showed the pathological change of fish liver tissue in the ND, HFD, and HFD+FSSB groups. Original magnification is ×200, bars, 50 μm. (d) Relative areas for lipid droplets in H&E staining. (e–g) TEM assay showed the alternations of ultrastructural of liver tissue in the ND, HFD, and HFD+FSSB groups. Original magnification is ×10,000, bars, 2 μm. Note: nu, hepatocyte nucleus; va, vacuole; ld, lipid droplet; mi, mitochondrial; er, endoplamic reticulum; gl, glycogen

KEGG pathway and protein expression pattern analysis

The KEGG database was used to identify potential biological pathways of DEPs. Between HFD+FSSB150 and HFD groups, the DEPs were mainly involved in geraniol degradation, butanoate metabolism, fat digestion and absorption, and the PPAR signaling pathway (Fig. 5a). Enrichment-based clustering of KEGG pathways showed that FA metabolism, fat digestion and absorption, cytochrome P450, the PPAR signaling pathway, geraniol degradation, and butanoate metabolism were downregulated in HFD-vs-ND, but they were upregulated in HFD+FSSB150-vs-HFD (Fig. 5b). To investigate the similarities and differences of DEPs' enriched pathways, the DEPs were classified into six clusters based on their expression levels. Proteins in clusters 1 to 3 showed low expression in the HFD group, while proteins in clusters 4 to 6 showed high expression in the HFD group. Additionally, peroxisome and carbon metabolism were highly ranked pathways in cluster 1. PPAR signaling pathway and oxidative phosphorylations were highly ranked pathways in cluster 2, which showed an equivalent protein expression level in ND and HFD+

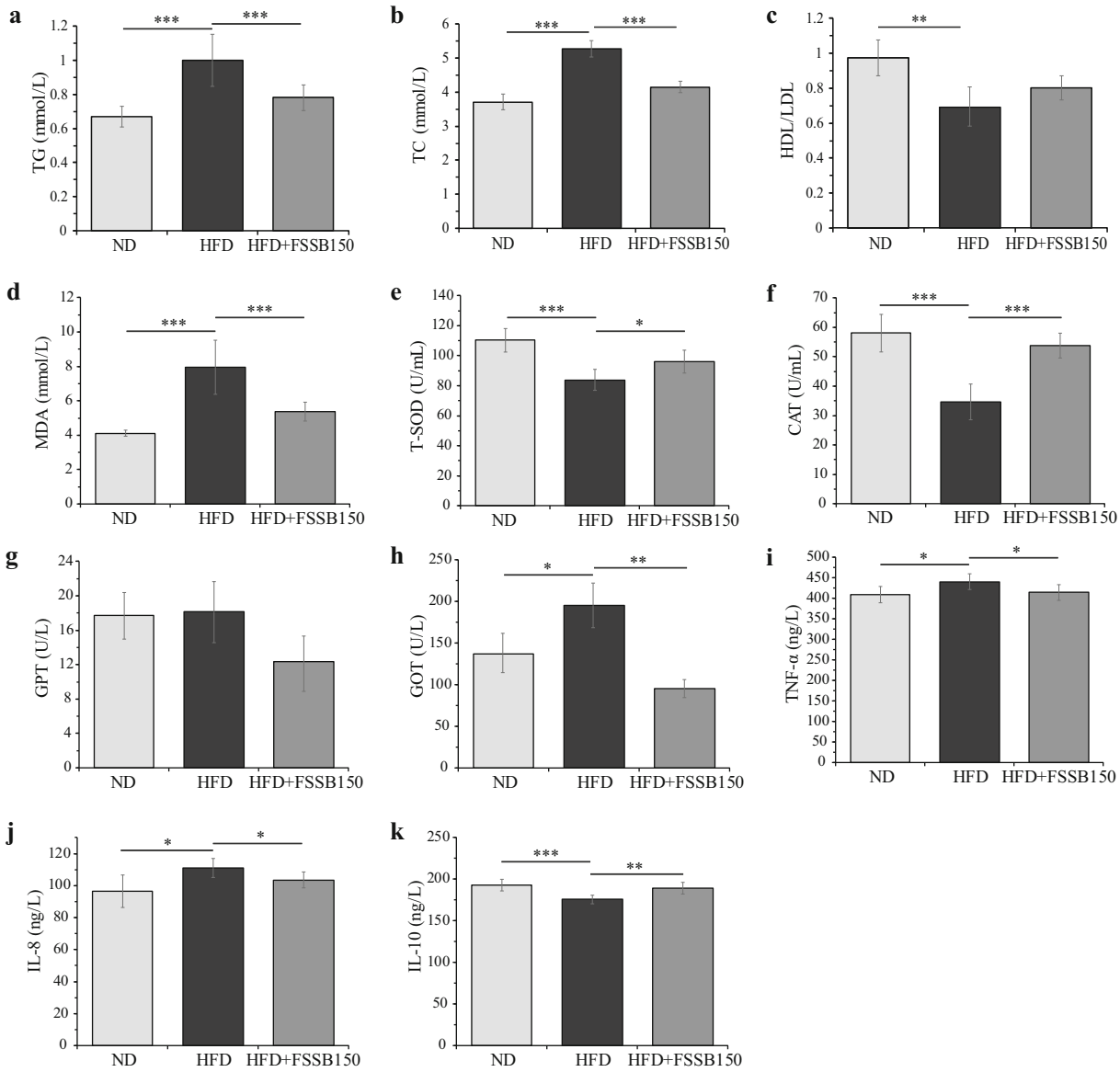

Fig. 2 FSSB attenuates lipid, oxidative, and inflammatory parameters of fatty liver disease induced by high-fat diet. (a, b) Serum contents of TG and TC in ND group, HFD group, and HFD+FSSB150 group. (c) Serum ratios of HDL/LDL in ND group, HFD group, and HFD+FSSB150 group. (d–f) Liver MDA level, T-SOD activity, and CAT activity in ND group, HFD group, and HFD+FSSB150 group. (g, h) Serum GPT and GOT activities in ND group, HFD group, and HFD+FSSB150 group. (i–k) Concentration of inflammatory cytokines TNF-α, IL-8, and IL-10 in ND group, HFD group, and HFD+FSSB150 group. *$p < 0.05$; **$p < 0.01$; ***$p < 0.001$

FSSB150 groups. Proteasome and ribosome pathways were highly ranked in cluster 3. Proteins in cluster 4 were equally expressed in ND and HFD+FSSB150, which were highly enriched in glycolysis/gluconeogenesis and carbon metabolism. Proteins in cluster 5 were mainly involved in proteasome and oxidative phosphorylation (Fig. 5c).

Dysregulated proteins involved in PPAR signaling pathway and fat digestion and absorption

KEGG pathway analysis showed that PPAR signaling pathway and fat digestion and absorption were involved in pathological process of fatty liver disease development. Besides, proteins involved in PPAR signaling

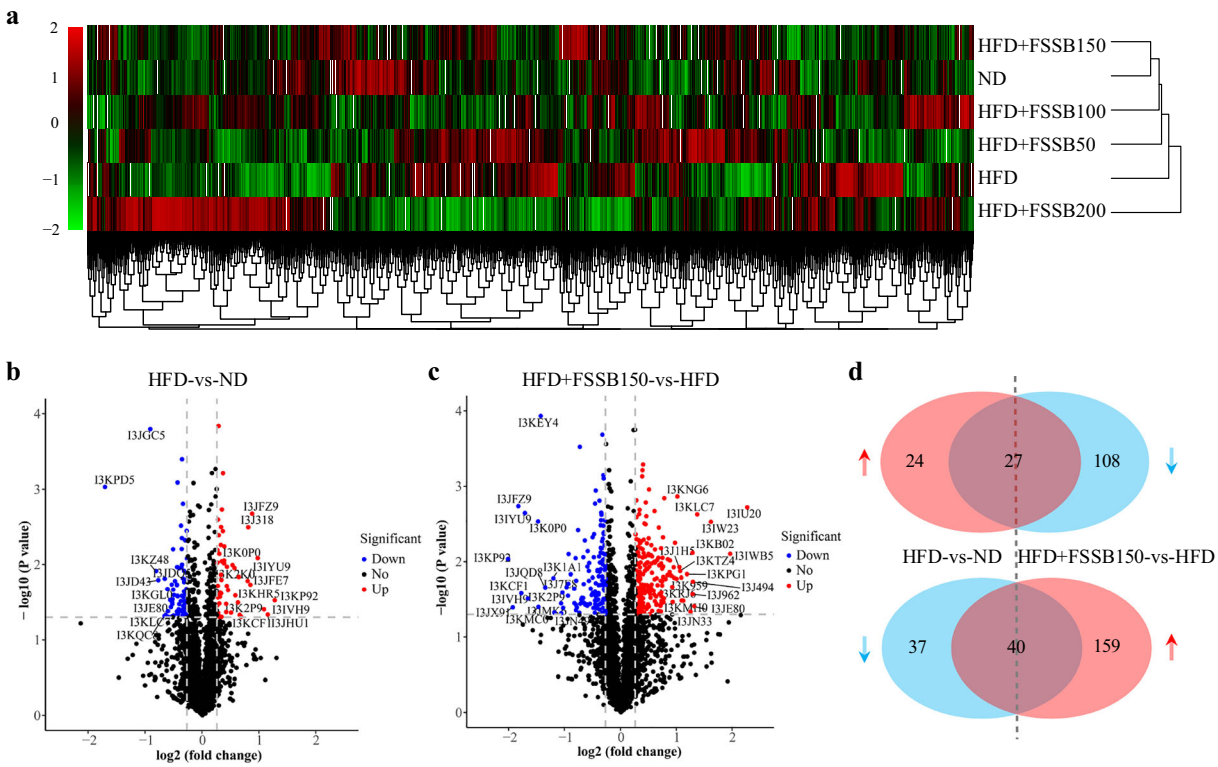

Fig. 3 Differential proteins expression analysis in livers of ND group, HFD group, and HFD supplied with different concentration gradients of FSSB. (a) The clustering heatmap of DEPs in ND group, HFD group, and HFD supplied with different concentration gradients of FSSB. Expression values are depicted in line with the color scale. The expression level enhancement increased from green to red. Each column represents one sample, and each row indicates a protein. (b, c) The volcano maps describe the number, significance, and reliability of DEPs in the comparison of HFD *vs.* ND and HFD+FSSB150 *vs.* HFD. Each dot represents one protein; red dots represent upregulated proteins and green dots represent downregulated proteins, while the gray dots represent proteins that are not differentially expressed between two groups. (d) Venn diagram containing four lists of upregulated and downregulated proteins between HFD *vs.* ND and HFD+FSSB150 *vs.* HFD

pathway, such as stearoyl-CoA desaturase (SCD1) and acyl-CoA-binding protein (ACBP), were downregulated in the HFD group compared to the ND group (Figure S1). However, after FSSB150 supplement in HFD, the expression of SCD1 and ACBP was reversed (Figure S2). Fatty acid-binding protein 1 (FABP1) and FABP3 were upregulated in the HFD+FSB150 group compared to the HFD group. Furthermore, proteins involved in fat digestion and absorption, such as apolipoprotein A-I (ApoA1), was downregulated in the HFD group compared to the ND group, and FSSB150 supplement reversed the expression of this protein.

Expression validation of GST, PPARs, and inflammatory cytokines

To further screen the key proteins related to fatty liver after SSB treatment, proteins with high fold change and high abundance were selected for further study. The expression level of four crucial genes such as glutathione S-transferase (*GST*), *PPARα*, *PPARβ*, and *PPARγ* that are involved in PPAR signaling pathway and fat digestion and absorption was validated by qRT-PCR. The expression of *GST* and PPARα showed significant decrease in the HFD group compared with the ND group, while their expression returned to the normal level after 150 mg/kg FSSB treatment (Fig. 6a). *PPARγ* showed remarkable high expression levels in the HFD group compared with the ND group. Conversely, supplementation of FSSB150 resulted in the significant decrease in the level of *PPARγ*. There was no significant difference in the expression of *PPARβ* among these groups. In addition, the expression of five inflammatory cytokine genes, including *TNF-α*, *IL-1β*, *IL-2*, *IL-6*, and *IL-8*, was also validated. In comparison with the ND group, the expression of *TNF-α*, *IL-1β*, *IL-6*, and *IL-8*

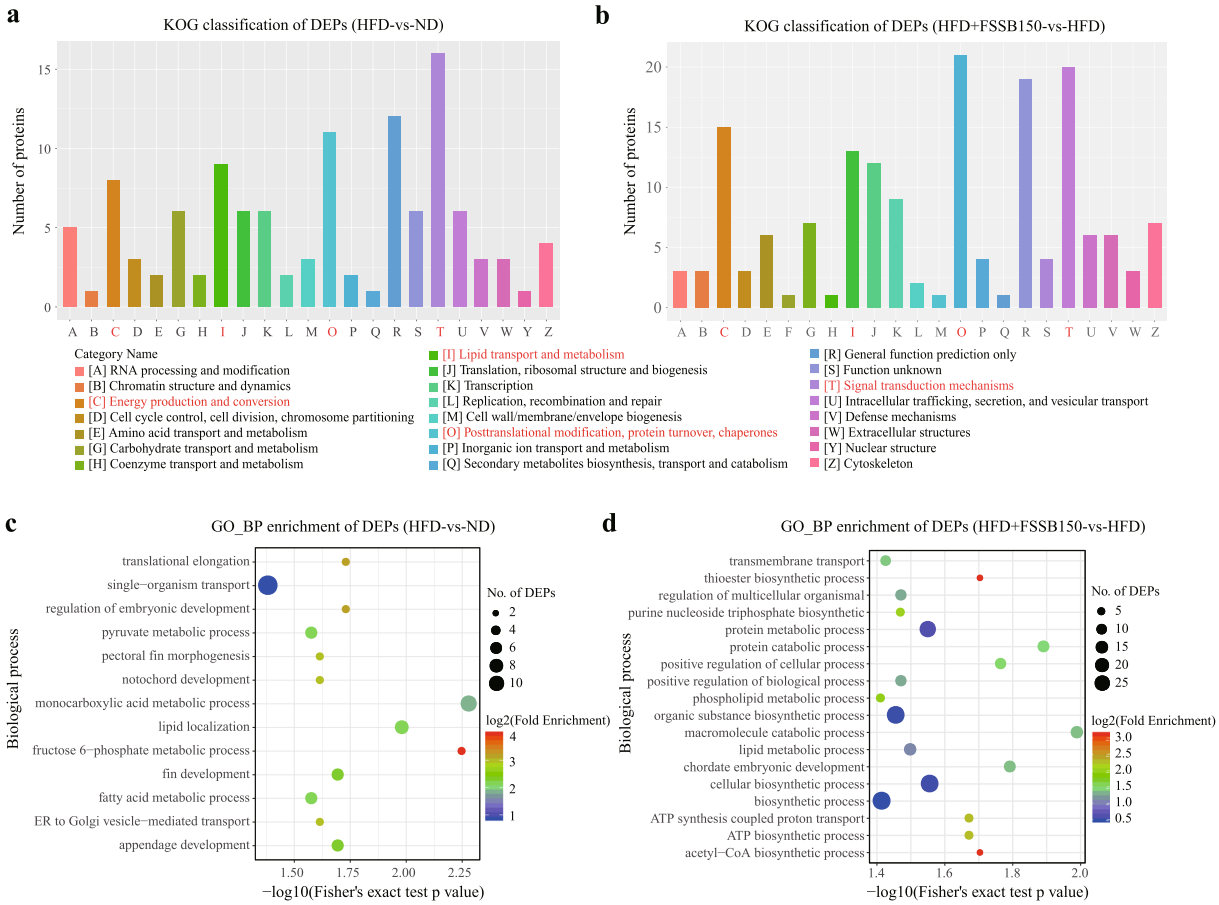

Fig. 4 The KOG and GO functional analysis of DEPs. (a, b) Column chart display significantly enriched KOG analysis of DEPs in liver tissue between HFD *vs.* ND and HFD+FSSB150 *vs.* HFD. (c) The bubble chart displays gene ontology biological process (GO_BP) analysis of DEPs in liver tissue between HFD *vs.* ND and HFD+FSSB150 *vs.* HFD. The change of bubbles from green to red means that the fold enrichment of function term is increased, and the size of bubble indicated that the number of proteins is enriched

was markedly increased, while IL-2 was significantly decreased in the HFD group. On the contrary, supplementation of FSSB150 reversed these changes (Fig. 6b).

Discussion

O. niloticus is an important economic fish species in China (Pan et al. 2017). Previous studies have reported that, with the common usage of HFD, numerous adverse effects such as reduced growth rate and disease resistance were observed in *O. niloticus* (Ning et al. 2017; Zhang et al. 2019). HFD can result in fatty liver disease in *O. niloticus*, which brings huge economic losses to the aquaculture industry (Tao et al. 2017); therefore, it is necessary to develop effective treatments. In this study, it was found that weight gain and specific growth rates were reduced in the HFD group compared to the ND group. However, the supplementation of FSSB150 in the HFD increased these indexes, indicating that FSSB could ameliorate the adverse effects of HFD on growth. Meanwhile, H&E staining showed that the liver tissues of the HFD group had aggravated swollen cells, obvious cavitation, vacuolar lipid droplets, and displaced nuclei compared to the ND group, suggesting the development of fatty liver disease. However, after supplement of FSSB150, the degree of cavitation was decreased and the liver tissues returned to relatively normal. These results indicated that FSSB could effectively prevent fatty liver disease in Nile tilapia.

Long-term feeding of HFD can result in abnormal liver function, which may lead to stress and thereby

Table 1 List of DEPs involved in acety-CoA metabolic process, ATP biosynthetic process, and lipid-related metabolic

Protein	Description	Gene name	HFD *vs.* NC		HFD+SSB150 *vs.* HFD		Functional classes
			Ratio	*p* value	Ratio	*p* value	
I3KK90	Hemopexin	*LOC100694811*	0.92	0.21	1.24	0.02	Response to lipid
I3JU54	Serine--pyruvate aminotransferase	*LOC100707770*	0.79	0	1.2	0.18	Response to lipid
I3J2Z4	Phosphoinositide 5-phosphatase	*ocrl*	1.25	0.07	0.76	0.03	Lipid metabolic process
I3JZ01	1-acyl-sn-glycerol-3-phosphate acyltransferase	*LOC100701022*	0.73	0.02	1.55	0.03	Fat digestion and absorption; lipid metabolic process
I3JX04	BPI1 domain-containing protein	*cetp*	1.35	0.02	1.23	0.06	Lipid transport
I3K835	Uncharacterized protein	*LOC100707019*	1.21	0	0.66	0.01	Lipid transport
I3JX91	Phosphoinositide phospholipase C	*plcg2*	1.66	0.12	0.26	0.04	Lipid metabolic process
I3K0G3	3-hydroxy-3-methylglutaryl coenzyme A synthase	*hmgcs1*	1.05	0.72	1.25	0.02	Lipid metabolic process
I3JR67	Uncharacterized protein	*ehhadh*	1.04	0.57	1.28	0.03	Lipid metabolic process
I3KJT9	Acetoacetyl-CoA synthetase	*aacs*	0.86	0.03	1.31	0	Lipid metabolic process
I3KEK2	Cytochrome b5 heme-binding domain-containing protein	*LOC100700077*	0.78	0.01	1.07	0.55	Lipid metabolic process
I3KLS8	Uncharacterized protein	*hadh*	0.77	0.03	1.4	0.04	Lipid metabolic process
I3JSU5	Fatty acid hydroxylase domain-containing protein	*sc5d*	0.69	0.02	1.89	0.05	Lipid metabolic process
I3JHL1	Sterol regulatory element-binding protein cleavage-activating protein	*scap*	0.66	0.05	1.64	0.05	Lipid metabolic process
I3KGL0	Stearoyl-CoA desaturase (delta-9-desaturase)	*scd*	0.65	0.02	1.29	0.14	Lipid metabolic process, PPAR signaling pathway
I3KGU7	Putative apolipoprotein A4b	*apoa4b*	0.9	0.14	1.21	0	Fat digestion and absorption; lipid transport
I3KIR4	Uncharacterized protein	*apoa4*	0.8	0.04	1.38	0.02	Fat digestion and absorption; lipid transport, PPAR signaling pathway
I3JEB1	Aspartate aminotransferase	*got2*	0.84	0.01	1.41	0.02	Fat digestion and absorption
I3J116	ATP synthase subunit d, mitochondrial	*atp5pd*	1.25	0.07	0.82	0.01	ATP biosynthetic process
D2KP28	ATP synthase protein 8	*atp8*	1.19	0.07	0.82	0.05	ATP biosynthetic process
I3K1D1	ATP synthase subunit beta	*LOC100693141*	0.8	0.03	1.69	0.12	ATP biosynthetic process
I3JE32	Diphosphomevalonate decarboxylase	*mvd*	0.84	0.02	1.56	0.01	Acyl-CoA metabolic process; lipid metabolic process
I3IXL2	ATP-citrate synthase	*acly*	0.86	0.02	1.31	0.01	Acyl-CoA metabolic process; lipid metabolic process
I3JC71	Pyruvate dehydrogenase E1 component subunit alpha	*LOC100709338*	0.72	0.02	1.39	0.01	Acyl-CoA metabolic process
I3KDH3	Uncharacterized protein	*fabp1*	0.99	0.92	1.23	0.02	Fat digestion and absorption, PPAR signaling pathway
I3KSU8	Carn_acyltransf domain-containing protein	*cpt2*	1.19	0.05	0.81	0	Fat digestion and absorption, PPAR signaling pathway
I3J1Z5	Uncharacterized protein	*fabp3*	0.78	0.1	1.4	0.04	PPAR signaling pathway
I3KLJ1	Uncharacterized protein	*dbi*	0.8	0.02	1.26	0.02	PPAR signaling pathway

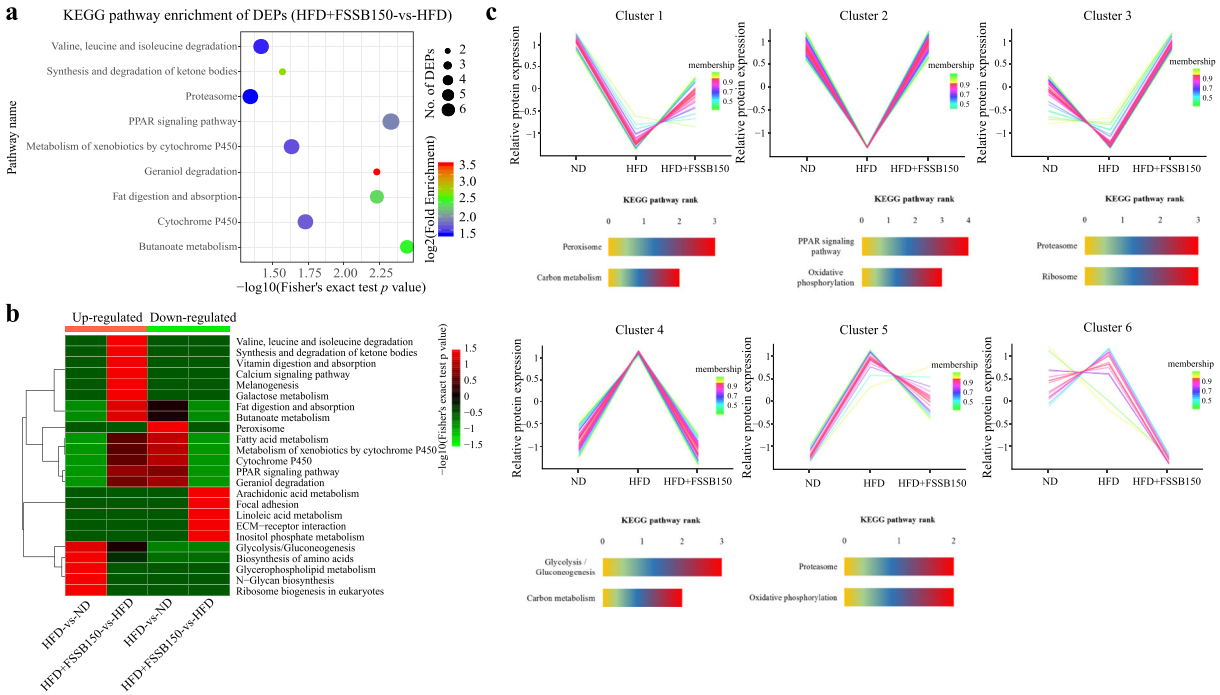

Fig. 5 The KEGG functional analysis of DEPs. (a) The bubble chart displays KEGG analysis of DEPs in liver tissue between HFD+FSSB150 *vs.* HFD. The change of bubbles from green to red means that the fold enrichment of function term is increased, and the size of bubble indicated that the number of proteins is enriched. (b) The clustering display significantly enriched KEGG pathways of upregulated and downregulated DEPs in HFD *vs.* ND and HFD+FSSB150 *vs.* HFD. (c) DEP expression pattern analysis and KEGG pathway enrichment of each cluster. The six clusters were classified of DEPs based on the expression level in ND group, HFD group, and HFD+FSSB150 group

causing fish disease and deaths. A previous study reported that blunt snout bream fed with HFD had increased TC and TG, indicating metabolic disorders of lipids and lipoproteins and liver damage (Adjoumani et al. 2017). In agreement with this result, in this study, supplementation of FSSB150 with HFD markedly decreased high levels of TG and TC caused by HFD, indicating that FSSB could improve lipid metabolism and have positive effect on growth of *O. niloticus*. In addition, excessive production of reactive oxygen species (ROS) indicates oxidative stress, which is also associated with liver damage in fish (Carine et al. 2019). SOD and CAT are known to detoxify ROS against oxidative stress and MDA is a key indicator of lipid oxidation rate as it reflects the level of cell damage (Shao et al. 2012; Christian et al. 2018). In the present study, it was observed that the level of MDA significantly decreased, and the activity of SOD and CAT significantly increased after FSSB150 supplementation, which indicated that FSSB might alleviate oxidative stress in fish liver tissues. Collectively, these results indicated that FSSB may reduce the adverse effects caused by HFD in *O. niloticus* through improving lipid metabolism and antioxidant ability.

Various pieces of evidence have demonstrated that flavanones have antiinflammatory effects in multiple organisms and have been used to treat multiple stresses (Choy et al. 2019; Owor et al. 2020). It was reported that HFD can promote the release of cytokines and induce inflammation in juvenile black seabream (*Acanthopagrus schlegelii*), which was verified in the present study (Jin et al. 2019). Our results showed that the expression levels of *TNF-α*, *IL-1β*, *IL-6*, and *IL-8* were significantly upregulated, whereas *IL-2* was markedly downregulated in the HFD group. In contrast, FSSB150 treatment reversed these changes. Similarly, a previous study showed that proinflammatory cytokines, such as *TNF-α*, *IL-1β*, *IL-8*, and *IL-6*, were remarkably increased in plasma and/or liver of tilapia fed with HFD (Jia et al. 2020). As an inflammatory mediator, *TNF-α* plays a critical role in the development of hepatic lipid disorder (Wang et al. 2016). Another study discovered that grape seed procyanidin extract dramatically reduced the expression of IL-6 and *TNF-α* in grass carp, suggesting that grape seed procyanidin extract might

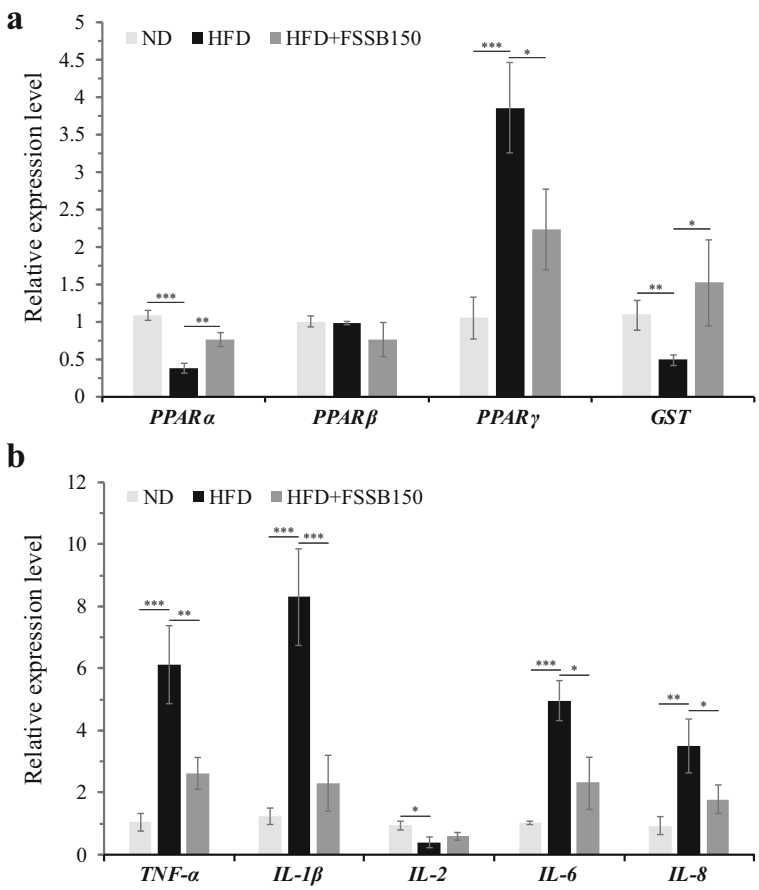

Fig. 6 Validation of *GST*, PPARs, and inflammatory factors. (a) Histogram showed that the expression of crucial genes *GST*, PPARs involved in PPAR signaling pathway. (b) Histogram showed that the expression of inflammatory cytokines *TNF-α*, *IL-1β*, *IL-2*, *IL-6*, and *IL-8*

regulate inflammatory response in fish through inhibiting pro-inflammatory cytokine production (Lu et al. 2020). Overall, these results verified the antiinflammatory effects of FSSB, which might contribute to the improvement of inflammatory response of HFD-induced fatty liver in Nile tilapia.

The PPAR signaling pathway is a well-known regulator of lipid metabolism, which involves three regulators: PPARα, PPARβ, and PPARγ. PPARα can accelerate oxidative lipid metabolism, and peroxisomal and mitochondrial FA β-oxidation (Mascaro et al. 1998; Miyazaki et al. 2004; Li et al. 2015). PPARβ and PPARγ also play crucial roles in both glucose and lipid metabolism, and have been shown to attenuate the severity of steatosis in mice (Nagasawa et al. 2006; Shan et al. 2008). In this study, the expression of PPARβ shows no significance among these groups, which was not consistent with our previous result (Huang et al. 2018b). We speculate that it may be affected by the breeding period or the repeatability of the biological detection. A recent study revealed that gemfibrozil supplementation can increase lipid catabolism and reduce lipogenesis through PPARα activation in Nile tilapia (Luo et al. 2020). In this study, qPCR analysis showed that FSSB150 significantly increased and decreased the expression levels of lower PPARα and higher PPARγ caused by HFD, respectively. Upregulation of *PPARα* and downregulation of *PPARγ* induced by FSSB might play a critical role in promoting oxidative lipid and peroxisome metabolism, as well as fat digestion and absorption, as these processes were found to have been enriched in our proteomic results. Moreover, we also found multiple proteins regulated by the PPAR signaling pathway such as ApoA1, SCD1, and ACBP. Overall, these results indicate that FSSB may alleviate fatty liver disease in Nile tilapia via the PPAR signaling pathway.

FABP1 is a cytoplasmic protein that desorbs long-chain fatty acids from membrane to cytoplasm and protects against the cytotoxicity of fatty acids by diffusing intracellular fatty acids (Huang et al. 2002; Meunier-Durmort et al. 1996). L-FABP was reported as a

diagnostic marker for non-alcoholic fatty liver disease because of its high levels in serum (Akbal et al. 2016). In this study, the proteomic analysis showed that FABP1 and FABP3 significantly increased in the HFD+ FSSB150 group compared to the HFD group, which may contribute to the utilization of intracellular fatty acid. Moreover, studies reported that overexpressed ApoA1 can protect against diet-induced fatty liver disease in mice (Karavia et al. 2012; McGrath et al. 2014) and rabbits (Wang et al. 2013). AopA1 was also involved in immune responses in carp (Concha et al. 2004), spotted sea bass (*Lateolabrax maculatus*) (Tian et al. 2019), and rainbow trout (Villarroel et al. 2007), especially against bacterial infection. In our study, FSSB could enhance the expression of downregulated ApoA1 induced by HFD. These results further indicate that FSSB may alleviate fatty liver disease in tilapia by reducing the risk of HFD-induced lipid accumulation.

Conclusion

Treatment with 150 mg/kg FSSB restored the physiological and pathological indexes to normal levels in tilapia with HFD-induced fatty liver disease. FSSB could improve the fatty liver by modulating fat digestion and absorption, and the PPAR signaling pathway. Additionally, *GST*, *PPAR*s, and multiple inflammatory cytokines regulated by FSSB might play a role in fatty liver disorders of tilapia. This study shows that FSSB is efficient for the treatment of nonalcoholic steatohepatitis at a 150 mg/kg dosage, thereby providing a new treatment strategy for nonalcoholic fatty liver disease in fish aquaculture.

Acknowledgements We thank the State Key Laboratory for Conservation and Utilization of Subtropical Agro-bioresources (SKLCUSA) for LC-MS/MS analysis.

Availability of data and material The data used to support the findings of this study are available from the corresponding author upon request.

Code availability Not applicable.

Author contribution K.H. and Z.T. proposed the idea and designed the experiments. K.Y. performed the proteomic experiment and participated in bioinformatics analysis. X.H. and L.S. prepared the animal materials and established the validation. L.P. and C.M. analyzed the original data. K.Y wrote the original manuscript. K.H revised and finalized the manuscript. All authors have read and approved the manuscript.

Funding This work was supported by the Natural Science Foundation of Guangxi Province, Grant/Award Number: No. 2018GXNSFDA281001; the Natural Science Foundation of Guangxi (Grant No. 2016GXNSFAA380233); and the Key Research and Development Projects of Guangxi, Grant/Award Number: No.AB18294011.

Declarations

Ethics approval This study was approved by the Animal Ethics Committee of Guangxi University.

Consent to participate Not applicable.

Consent for publication Not applicable.

Conflict of interest The authors declare no competing interests.

References

Adjoumani JY, Wang K, Zhou M, Liu W, Zhang D (2017) Effect of dietary betaine on growth performance, antioxidant capacity and lipid metabolism in blunt snout bream fed a high-fat diet. Fish Physiol Biochem 43:1733–1745. https://doi.org/10.1007/s10695-017-0405-9

Akbal E, Kocak E, Akyurek O, Koklu S, Batgi H, Senes M (2016) Liver fatty acid-binding protein as a diagnostic marker for non-alcoholic fatty liver disease. Wien Klin Wochenschr 128:48–52. https://doi.org/10.1007/s00508-014-0680-8

Carine DFS, Baldissera MD, Verdi CM, Santos RCV, Da Rocha MIUM, Da Veiga ML, Da Silva AS, Baldisserotto B (2019) Oxidative stress and antioxidant responses in Nile tilapia *Oreochromis niloticus* experimentally infected by *Providencia rettgeri*. Microb Pathog 131:164–169. https://doi.org/10.1016/j.micpath.2019.04.007

Choy KW, Murugan D, Leong XF, Abas R, Alias A, Mustafa MR (2019) Flavonoids as natural anti-inflammatory agents targeting nuclear Factor-Kappa B (NFkappaB) signaling in cardiovascular diseases: a mini review. Front Pharmacol 10:1295. https://doi.org/10.3389/fphar.2019.01295

Christian LA, Jinliang Z, Jun-Wei W, Loor JJ (2018) Replacement of fish oil with palm oil: effects on growth performance, innate immune response, antioxidant capacity and disease resistance in Nile tilapia (*Oreochromis niloticus*). PLoS One 13:e0196100. https://doi.org/10.1371/journal.pone.0196100

Concha MI, Smith VJ, Castro K, Bastias A, Romero A, Amthauer RJ (2004) Apolipoproteins A-I and A-II are potentially important effectors of innate immunity in the teleost fish *Cyprinus carpio*. Eur J Biochem 271:2984–2990. https://doi.org/10.1111/j.1432-1033.2004.04228.x

Du J, Jia R, Cao LP, Ding W, Xu P, Yin G (2018) Effects of *Rhizoma Alismatis* extract on biochemical indices and

adipose gene expression in oleic acid-induced hepatocyte injury in Jian carp (*Cyprinus carpio* var. Jian). Fish Physiol Biochem 44:747–768. https://doi.org/10.1007/s10695-017-0428-2

Fan JG (2010) Guidelines for management of nonalcoholic fatty liver disease: an updated and revised edition. Chin J Hepatol 14(3):163–166

Furuhashi M, Hotamisligil GS (2008) Fatty acid-binding proteins: role in metabolic diseases and potential as drug targets. Nat Rev Drug Discov 7:489–503. https://doi.org/10.1038/nrd2589

Goessling W, Sadler KC (2015) Zebrafish: an important tool for liver disease research. Gastroenterology 149:1361–1377. https://doi.org/10.1053/j.gastro.2015.08.034

He A, Wang M, Hao H, Zhang D, Lee K-H (1998) Hepatoprotective triterpenes from Sedum sarmentosum. Phytochem 49:2607–2610

Huang H., Starodub O., McIntosh A., Kier A.B., Schroeder F., 2002. Liver fatty acid-binding protein targets fatty acids to the nucleus. Real time confocal and multiphoton fluorescence imaging in living cells. J Biol Chem 277, 29139-29151. https://doi.org/10.1074/jbc.M202923200

Huang FF, Wang JJ, Yu FM, Tang YP, Ding GF, Yang ZS, Sun Y (2018a) Protective effect of Meretrix meretrix oligopeptides on high-fat-diet-induced non-alcoholic fatty liver disease in mice. Mar Drugs 16(2):39. https://doi.org/10.3390/Md16020039

Huang L, Cheng Y, Huang K, Zhou Y, Ma Y, Zhang M (2018b) Ameliorative effect of *Sedum sarmentosum* Bunge extract on tilapia fatty liver via the PPAR and P53 signaling pathway. Sci Rep 8:8456. https://doi.org/10.1038/s41598-018-26084-2

Jia Y, Jing Q, Niu H, Huang B (2017) Ameliorative effect of vitamin E on hepatic oxidative stress and hypoimmunity induced by high-fat diet in turbot (*Scophthalmus maximus*). Fish Shellfish Immunol 67:634–642. https://doi.org/10.1016/j.fsi.2017.06.056

Jia R, Cao LP, Du JL, He Q, Gu ZY, Jeney G, Xu P, Yin GJ (2020) Effects of high-fat diet on antioxidative status, apoptosis and inflammation in liver of tilapia (*Oreochromis niloticus*) via Nrf2, TLRs and JNK pathways. Fish Shellfish Immunol 104:391–401. https://doi.org/10.1016/j.fsi.2020.06.025

Jin M, Pan T, Tocher DR, Betancor MB, Monroig Ó, Shen Y, Zhu T, Sun P, Jiao L, Zhou Q (2019) Dietary choline supplementation attenuated high-fat diet-induced inflammation through regulation of lipid metabolism and suppression of NF-κB activation in juvenile black seabream (*Acanthopagrus schlegelii*). J Nutr Sci 8:e38. https://doi.org/10.1017/jns.2019.34

Karavia EA, Papachristou DJ, Liopeta K, Triantaphyllidou IE, Dimitrakopoulos O, Kypreos KE (2012) Apolipoprotein A-I modulates processes associated with diet-induced nonalcoholic fatty liver disease in mice. Mol Med 18:901–912. https://doi.org/10.2119/molmed.2012.00113

Kitade H, Chen G, Ni Y, Ota T (2017) Nonalcoholic fatty liver disease and insulin resistance: new insights and potential new treatments. Nutrients 9(4):387. https://doi.org/10.3390/nu9040387

Landgraf K, Schuster S, Meusel A, Garten A, Riemer T, Schleinitz D, Kiess W, Korner A (2017) Short-term overfeeding of zebrafish with normal or high-fat diet as a model for the development of metabolically healthy versus unhealthy obesity. BMC Physiol 17(1):4. https://doi.org/10.1186/s12899-017-0031-x

Lau JKC, Zhang X, Yu J (2017) Animal models of non-alcoholic fatty liver disease: current perspectives and recent advances. J Pathol 241:36–44. https://doi.org/10.1002/path.482

Li J, Huang Q, Long X, Zhang J, Huang X, Aa J, Yang H, Chen Z, Xing J (2015) CD147 reprograms fatty acid metabolism in hepatocellular carcinoma cells through Akt/mTOR/SREBP1c and P38/PPARalpha pathways. J Hepatol 63:1378–1389. https://doi.org/10.1016/j.jhep.2015.07.039

Lieschke GJ, Currie PD (2007) Animal models of human disease: zebrafish swim into view. Nat Rev Genet 8:353–367. https://doi.org/10.1038/nrg2091

Lin Y, Luo H, Liu H, Du X (2020) Anti-fibrotic mechanism of *Sedum sarmentosum* total flavanones in inhibiting activation of HSC by regulating Smads. China J Chin Mater Med 45(3):631–635. https://doi.org/10.19540/j.cnki.cjcmm.20190829.401

Lu RH, Qin CB, Yang F, Zhang WY, Zhang YR, Yang GK, Yang LP, Meng XL, Yan X, Nie GX (2020) Grape seed proanthocyanidin extract ameliorates hepatic lipid accumulation and inflammation in grass carp (*Ctenopharyngodon idella*). Fish Physiol Biochem 46(5):1665–1677. https://doi.org/10.1007/s10695-020-00819-3

Luo Y, Hu CT, Qiao F, Wang XD, Qin JG, Du ZY, Chen LQ (2020) Gemfibrozil improves lipid metabolism in Nile tilapia *Oreochromis niloticus* fed a high-carbohydrate diet through peroxisome proliferator activated receptor-α activation. Gen Comp Endocrinol 296:113537. https://doi.org/10.1016/j.ygcen.2020.113537

Mascaro C, Acosta E, Ortiz JA, Marrero PF, Hegardt FG, Haro D (1998) Control of human muscle-type carnitine palmitoyltransferase I gene transcription by peroxisome proliferator-activated receptor. J Biol Chem 273:8560–8563. https://doi.org/10.1074/jbc.273.15.8560

Matsumoto T, Terai S, Oishi T, Ku Washiro S, Fujisawa K, Yamamoto N, Fujita Y, Hamamoto Y, Furutani-Seiki M, Nishina H, Sakaida I (2010) Medaka as a model for human nonalcoholic steatohepatitis. Dis Model Mech 3:431–440. https://doi.org/10.1242/dmm.002311

McGrath KC, Li XH, Whitworth PT, Kasz R, Tan JT, McLennan SV, Celermajer DS, Barter PJ, Rye KA, Heather AK (2014) High density lipoproteins improve insulin sensitivity in high-fat diet-fed mice by suppressing hepatic inflammation. J Lipid Res 55:421–430. https://doi.org/10.1194/jlr.M043281

Meunier-Durmort C, Poirier H, Niot I, Forest C, Besnard P (1996) Up-regulation of the expression of the gene for liver fatty acid-binding protein by long-chain fatty acids. Biochem J 319(Pt 2):483–487. https://doi.org/10.1042/bj3190483

Miyazaki M, Dobrzyn A, Sampath H, Lee SH, Man WC, Chu K, Peters JM, Gonzalez FJ, Ntambi JM (2004) Reduced adiposity and liver steatosis by stearoyl-CoA desaturase deficiency are independent of peroxisome proliferator-activated receptor-alpha. J Biol Chem 279:35017–35024. https://doi.org/10.1074/jbc.M405327200

Nagasawa T, Inada Y, Nakano S, Tamura T, Takahashi T, Maruyama K, Yamazaki Y, Kuroda J, Shibata N (2006) Effects of bezafibrate, PPAR pan-agonist, and GW501516, PPARdelta agonist, on development of steatohepatitis in mice fed a methionine- and choline-deficient diet. Eur J

Pharmacol 536:182–191. https://doi.org/10.1016/j.ejphar.2006.02.028

Ning LJ, He AY, Lu DL, Li JM, Qiao F, Li DL, Zhang ML, Chen LQ, Du ZY (2017) Nutritional background changes the hypolipidemic effects of fenofibrate in Nile tilapia (*Oreochromis niloticus*). Sci Rep 7:41706. https://doi.org/10.1038/srep41706

Owor RO, Bedane KG, Zuhlke S, Derese S, Ong'amo GO, Ndakala A, Spiteller M (2020) Anti-inflammatory flavanones and flavones from *Tephrosia linearis*. J Nat Prod 83:996–1004. https://doi.org/10.1021/acs.jnatprod.9b00922

Pan H, Li LY, Li JM, Wang WL, Limbu SM, Degrace P, Li DL, Du ZY (2017) Inhibited fatty acid beta-oxidation impairs stress resistance ability in Nile tilapia (*Oreochromis niloticus*). Fish Shellfish Immunol 68:500–508. https://doi.org/10.1016/j.fsi.2017.07.058

Prisingkorn W, Prathomya P, Jakovlic I, Liu H, Zhao YH, Wang WM (2017) Transcriptomics, metabolomics and histology indicate that high-carbohydrate diet negatively affects the liver health of blunt snout bream (*Megalobrama amblycephala*). BMC Genomics 18:856. https://doi.org/10.1186/s12864-017-4246-9

Qiang J, Tao YF, Bao JW, Chen J, Li HX, He J, Xu P (2018) High fat diet-induced miR-122 regulates lipid metabolism and fat deposition in genetically improved farmed Tilapia (GIFT, *Oreochromis niloticus*) Liver. Front Physiol 9:1422. https://doi.org/10.3389/fphys.2018.01422

Shan W, Nicol CJ, Ito S, Bility MT, Kennett MJ, Ward JM, Gonzalez FJ, Peters JM (2008) Peroxisome proliferator-activated receptor-beta/delta protects against chemically induced liver toxicity in mice. Hepatology 47:225–235. https://doi.org/10.1002/hep.21925

Shao XP, Liu WB, Lu KL, Xu WN, Zhang WW, Wang Y, Zhu J (2012) Effects of tribasic copper chloride on growth, copper status, antioxidant activities, immune responses and intestinal microflora of blunt snout bream (*Megalobrama amblycephala*) fed practical diets. Aquaculture 338-341:154–159. https://doi.org/10.1016/j.aquaculture.2012.01.018

Tao YF, Qiang J, Yin GJ, Xu P, Shi Q, Bao JW (2017) Identification and characterization of lipid metabolism-related microRNAs in the liver of genetically improved farmed tilapia (GIFT, *Oreochromis niloticus*) by deep sequencing. Fish Shellfish Immunol 69:227–235. https://doi.org/10.1016/j.fsi.2017.08.023

Tao YF, Qiang J, Bao JW, Chen DJ, Yin GJ, Xu P, Zhu HJ (2018) Changes in physiological parameters, lipid metabolism, and expression of microRNAs in genetically improved farmed Tilapia (*Oreochromis niloticus*) with fatty liver induced by a high-fat diet. Front Physiol 9:1521. https://doi.org/10.3389/fphys.2018.01521

Tian J, Wu F, Yang CG, Jiang M, Liu W, Wen H (2015) Dietary lipid levels impact lipoprotein lipase, hormone-sensitive lipase, and fatty acid synthetase gene expression in three tissues of adult GIFT strain of Nile tilapia, *Oreochromis niloticus*. Fish Physiol Biochem 41:1–18. https://doi.org/10.1007/s10695-014-0001-1

Tian Y, Wen H, Qi X, Mao X, Shi Z, Li J, He F, Yang W, Zhang X, Li Y (2019) Analysis of apolipoprotein multigene family in spotted sea bass (*Lateolabrax maculatus*) and their expression profiles in response to vibrio harveyi infection. Fish Shellfish Immunol 92:111–118. https://doi.org/10.1016/j.fsi.2019.06.005

Villarroel F, Bastias A, Casado A, Amthauer R, Concha MI (2007) Apolipoprotein A-I, an antimicrobial protein in *Oncorhynchus mykiss*: evaluation of its expression in primary defence barriers and plasma levels in sick and healthy fish. Fish Shellfish Immunol 23:197–209. https://doi.org/10.1016/j.fsi.2006.10.008

Wang W, Zhou W, Wang B, Zhu H, Ye L, Feng M (2013) Antioxidant effect of apolipoprotein A-I on high-fat diet-induced non-alcoholic fatty liver disease in rabbits. Acta Biochim Biophys Sin Shanghai 45:95–103. https://doi.org/10.1093/abbs/gms100

Wang JW, Chen XY, Hu PY, Tan MM, Tang XG, Huang MC, Lou ZH (2016) Effects of *Linderae radix* extracts on a rat model of alcoholic liver injury. Exp Ther Med 11:2185–2192. https://doi.org/10.3892/etm.2016.3244

Zhang D, Lu K, Dong Z, Jiang G, Xu W, Liu W (2014) The effect of exposure to a high-fat diet on microRNA expression in the liver of blunt snout bream (*Megalobrama amblycephala*). PLoS One 9:e96132. https://doi.org/10.1371/journal.pone.0096132

Zhang YX, Jiang ZY, Han SL, Li LY, Du ZY (2019) Inhibition of intestinal lipases alleviates the adverse effects caused by high-fat diet in Nile tilapia. Fish Physiol Biochem:46. https://doi.org/10.1007/s10695-019-00701-x

Zuo RT, Ai QH, Mai KS, Xu W, Wang J, Xu HG, Liufu ZG, Zhang YJ (2012) Effects of dietary n-3 highly unsaturated fatty acids on growth, nonspecific immunity, expression of some immune related genes and disease resistance of large yellow croaker (*Larmichthys crocea*) following natural infestation of parasites (*Cryptocaryon irritans*). Fish Shellfish Immunol 32:249–258. https://doi.org/10.1016/j.fsi.2011.11.005